

Low-Cost, Smartphone-Based Specular Imaging and Automated Analysis of the Corneal Endothelium

Sreekar Mantena^{1,2,*}, Jay Chandra^{1,2,*}, Eryk Pecyna^{1,2}, Andrew Zhang^{1,2}, Dominic Garrity^{1,2}, Stephan Ong Tone^{3-5,8}, Srinivas Sastry⁶, Madhu Uddaraju⁷, and Ula V. Jurkunas³⁻⁵

¹ Harvard John A. Paulson School of Engineering and Applied Science, Cambridge, MA, USA

² Global Alliance for Medical Innovation, Cambridge, MA, USA

³ Cornea Center of Excellence, Schepens Eye Research Institute, Harvard Medical School, Boston, MA, USA

⁴ Massachusetts Eye and Ear Infirmary, Harvard Medical School, Boston, MA, USA

⁵ Department of Ophthalmology, Harvard Medical School, Boston, MA, USA

⁶ Bethesda Retina, Bethesda, MD, USA

⁷ Sri Kiran Institute of Ophthalmology, Kakinada, Andhra Pradesh, India

⁸ Sunnybrook Health Sciences Centre and Sunnybrook Research Institute, Department of Ophthalmology and Vision Sciences, University of Toronto, Toronto, Ontario, Canada

Correspondence: Ula V. Jurkunas, Cornea Center of Excellence, Department of Ophthalmology, Harvard Medical School, Schepens Eye Research Institute, 20 Staniford Street, Boston, 02114-MA, USA. e-mail:

ula_jurkunas@meei.harvard.edu

Received: December 4, 2020

Accepted: February 11, 2021

Published: April 2, 2021

Keywords: corneal endothelial cells; specular microscopy; corneal development; smartphone

Citation: Mantena S, Chandra J, Pecyna E, Zhang A, Garrity D, Ong Tone S, Sastry S, Uddaraju M, Jurkunas UV. Low-cost, smartphone-based specular imaging and automated analysis of the corneal endothelium. *Trans Vis Sci Tech.* 2021;10(4):4. <https://doi.org/10.1167/tvst.10.4.4>

Purpose: Specular and confocal microscopes are important tools to monitor the health of the corneal endothelium (CE), but their high costs significantly limit accessibility in low-resource environments. We developed and validated a low-cost, fully automated method to quantitatively evaluate the CE using smartphone-based specular microscopy.

Methods: A OnePlus 7 Pro smartphone attached to a Topcon SL-D701 slit-lamp was used to image the central corneal endothelium of 30 eyes using the specular reflection technique. A novel on-device image processing algorithm automatically computed endothelial cell density (ECD), percentage of hexagonal cells (HEX), and coefficient of variation (CV) values. These values were compared with the ECD, HEX, and CV generated by a Tomey EM-4000 specular microscope used to image the same set of eyes.

Results: No significant differences were found in ECD (2799 ± 156 cells/mm² vs. 2779 ± 166 cells/mm²; $P = 0.28$) and HEX ($52 \pm 6\%$ vs. $53 \pm 6\%$; $P = 0.50$) computed by smartphone-based specular imaging and specular microscope, respectively. A statistically significant difference in CV ($34 \pm 3\%$ vs. $30 \pm 3\%$; $P < 0.01$) was found between the two methods. The concordance achieved between the smartphone-based method and the Tomey specular microscope is very similar to the concordance between two specular microscopes reported in the literature.

Conclusions: Smartphone-based specular imaging and automated analysis is a low-cost method to quantitatively evaluate the CE with accuracy comparable to the clinical standard.

Translational Relevance: This tool can be used to screen the CE in low-resource regions and prompt investigation of suspected corneal endotheliopathies.

Introduction

The corneal endothelium (CE) is located on the posterior corneal surface and plays a key role in maintaining the cornea in a state of relative dehydration by acting as a selective leaky barrier and an active

metabolic pump, which helps to maintain its optical transparency.¹ The CE is composed of a monolayer of hexagonally shaped cells that rest on a specialized membrane called Descemet's membrane. Proper size, shape, and cell density of the CE are vital to maintaining the corneal hydration balance and are indicative of CE function. The integrity of the CE

can be compromised by primary corneal endotheliopathies, such as Fuchs endothelial corneal dystrophy (FECD), or secondary endotheliopathies due to intraocular surgery, such as cataract surgery. Data collected from a national managed-care network in the United States found an approximate prevalence of 897 cases of endothelial disease per 100,000 people, 60.4% of which were attributed to FECD.^{2,3} Unmanaged corneal endotheliopathies can lead to corneal edema and vision loss.

The ability to evaluate the morphological characteristics of the CE is critical to diagnosing and monitoring patients with corneal diseases. Currently, specular microscopy (both contact and non-contact) and in vivo confocal microscopy are capable of imaging the CE and allow for morphometric analysis.⁴ These commercially available microscopes automatically determine endothelial cell density (ECD), the percentage of cells which are hexagonal (HEX), and coefficient of variation (CV), which are important parameters in evaluating the CE. However, these microscopes have high operation costs (\$25,000 to \$30,000), which limit accessibility in resource-scarce settings. Although this is especially significant for developing countries, even in the United States, specular microscopes are prohibitively expensive for many medical practices due to the limited indications for which Medicare provides reimbursement.⁵ Therefore, there is a need for a low-cost and reliable method to image and evaluate the CE.

Smartphone-based specular microscopy has been described as a low-cost technique to image the CE at subcellular resolution.⁶ This method uses a smartphone attached to a slit-lamp ocular and utilizes the specular reflection technique to image the CE. However, this method has not been validated or compared to currently available specular microscopes. Furthermore, prior studies required manual cell annotation of smartphone-based specular images by trained ophthalmologists, making this technique labor-intensive and limiting its ability to be deployed in a clinical setting.⁷

Automated analysis of smartphone-based CE images would make this technique clinically feasible. However, this analysis is a complex image processing task. Uneven illumination across the image, the presence of artifacts, and low resolution are all factors which make segmentation of cell borders and subsequent calculation of ECD, HEX, and CV very challenging.⁸ Images acquired via smartphone-based specular microscopy are even more difficult to analyze than those obtained using a traditional specular microscope, as they have lower resolution and more noise.

Over the past 2 decades, many researchers have proposed image processing methods to accurately

segment cell borders and compute the morphological parameters of endothelial cells. Recent papers have described segmentation methods based on convolutional neural networks (CNNs), which have the potential to be more accurate than traditional techniques.⁹ However, these methods require a very large training dataset with corresponding ground truths, in which cell borders need to be manually delineated by ophthalmologists.

Many traditional segmentation approaches are based on the Krzysztof Habrat (KH) algorithm, which uses directional filtering to identify cell borders.⁸ We built a novel image processing pipeline that combines the KH segmentation algorithm with light normalization, denoising, and artifact removal techniques to enable accurate analysis of smartphone-based specular images. Our platform computes clinically relevant parameters, such as ECD, HEX, and CV, and the complete analysis can be run in under 5 seconds on a mobile device, without the need for an internet connection.

In this study, we describe a smartphone-based CE imaging technique and our fully automated analysis pipeline and validate it against the clinical standard. We compare morphometric analysis parameters from healthy participants as determined by our smartphone-based analysis to those reported by a commercially available non-contact specular microscope.

Materials and Methods

Data Acquisition

This study was conducted at the Sri Kiran Institute of Ophthalmology, a referral eye hospital in Andhra Pradesh, India, with examination dates between January 2, 2020, and January 9, 2020. This study was approved by the Institutional Review Board of the Sri Kiran Institute of Ophthalmology and was in compliance with the Declaration of Helsinki. Informed written consent was obtained from all participants.

We recruited 15 healthy human subjects without known ocular diseases. All participants enrolled were individuals who had appeared for a routine eye examination.

The central cornea of both eyes of each participant was imaged using the Tomey EM-4000 specular microscope (Tomey Corporation, Phoenix, AZ, USA). The ECD, HEX, and CV values outputted by the specular microscope were recorded. Subsequently, images were acquired using a smartphone (OnePlus 7 Pro; OnePlus Technology, Shenzhen, China) fastened to one ocular of a Topcon SL-D701 slit-lamp (TopCon



Figure 1. Imaging setup of smartphone-based method. OnePlus 7 Pro smartphone is shown attached to the Topcon slit lamp.

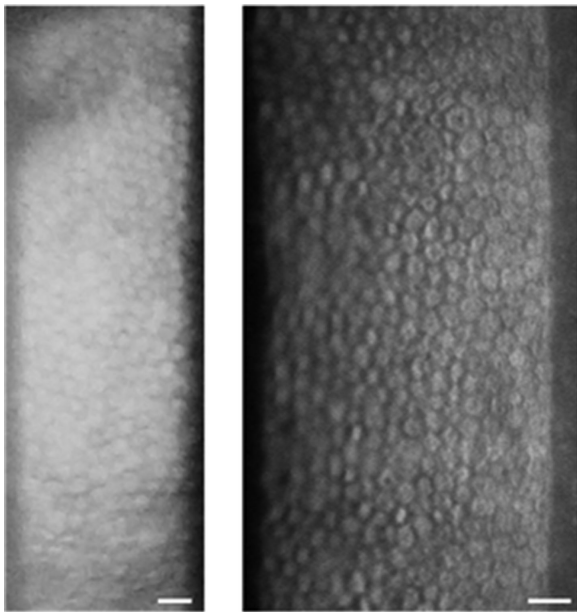


Figure 2. Comparison of corneal endothelial images captured by smartphone-based imaging (*left*) and captured by the Tomy specular microscope (*right*). Both images show the characteristic honeycomb pattern of the corneal endothelium. Scale bar: 50 μm .

Corporation, Tokyo, Japan) using a smartphone-telescope adapter mount (Gosky Optics, Atlanta, GA, USA), as shown in [Figure 1](#). The specular reflection technique was used to capture the CE at subcellular resolution. The height and width of the slit-lamp beam were adjusted to 4 mm and 2 mm, respectively. The light source was positioned 45 degrees relative to the optical axis of the slit-lamp, the ocular was adjusted to 40 \times zoom, and the backlight was placed on the lowest brightness setting. An ISO of 800 and shutter

speed of 1/125 were used to capture images of the CE. The smartphone was manually focused until the characteristic hexagonal pattern of the CE was clearly visible, and the image was captured. A technician performed all imaging, and the total capture and analysis process took approximately 2 to 4 minutes for both eyes.

An example image acquired using this smartphone-based method and the corresponding image of the same eye captured using the Topcon specular microscope is displayed in [Figure 2](#). The smartphone app user workflow is represented in [Figure 3](#).

Image Processing

In order to analyze the image and compute morphological parameters, we developed an image processing pipeline, which consists of eight steps: grayscale conversion, light normalization, image smoothing, KH segmentation, image binarization, thinning of border lines, artifact removal, and triple-point analysis. Each step of the process is displayed in [Figure 4](#).

Preprocessing

The image was first converted to grayscale, such that each pixel was stored as a value from 0 to 255. A smoothing method was applied to average the pixel values in a radius of three pixels to reduce image noise, remove artifacts, and amplify cell borders. Next, an algorithm was applied to normalize uneven illumination in the image. The technique adjusts pixel values in the image such that any given neighborhood of radius 16 pixels has approximately the same average brightness as the average brightness of the entire image.

Segmentation

Once the two preprocessing steps were complete, the image underwent segmentation by a directional-filtering (KH) algorithm.⁸ Four masks were applied to the original image, and the resulting four images were merged to generate the final segmentation. However, occasionally cell nuclei still remained in the segmented images, disrupting further analysis. An artifact removal algorithm was applied to remove any objects less than 40 pixels in the area, successfully filtering out both processing artifacts and nuclei.

A flood-based iterative thinning algorithm was used to thin all the cell borders in order to facilitate

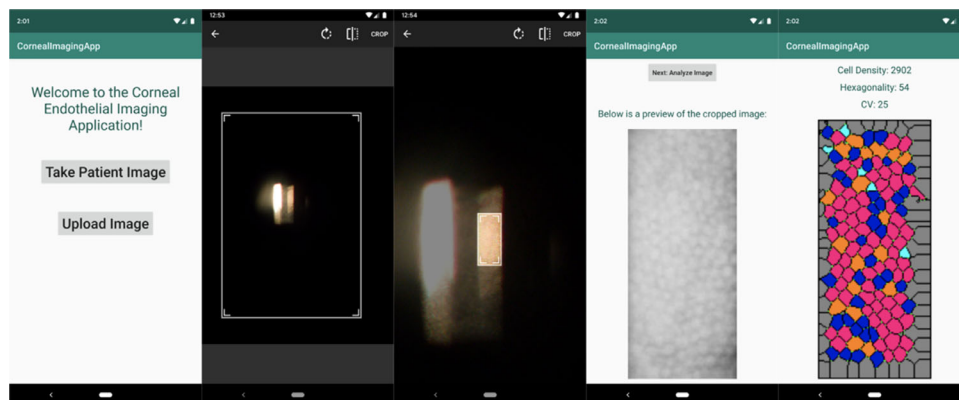


Figure 3. Image acquisition and analysis using smartphone application. (A) User can upload or take image. (B) Crop image and select subsection for analysis. (C) Preview of image to be processed. (D) Results of analysis, including endothelial cell density (ECD), cell hexagonality (HEX), and cell variation (CV). Segmented image is displayed, with cyan cells being four-sided, blue cells being five-sided, pink cells being six-sided, orange cells being seven-sided, and white cells being eight-sided or more.

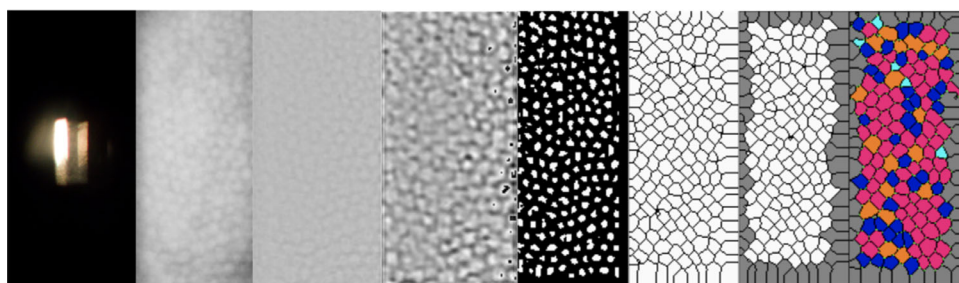


Figure 4. Image analysis processing pipeline. Left to Right: Raw Image, Cropped Image, Light Normalization, Smoothing, KH Algorithm, Thinning, Artifact Removal, and Triple-Point Analysis.

parameter calculation.⁸ A set of three by three masks were repeatedly applied to the segmented image, resulting in cell borders, which are a single pixel wide.

Parameter Calculation

In order to quantify cell shape, we used a triple point analysis technique.¹⁰ We identified the number of three-line intersections (triple points) that surround the cell, which is equivalent to the number of sides of a cell. Cell hexagonality was defined as the number of hexagonal cells divided by the total number of cells.

The cell density calculation was computed by counting the number of cells in the image and dividing by the actual size of the image (in mm^2). The image size was inferred by the equation below, where M_s is the magnification of the slit-lamp microscope, f_c is the focal length of the OnePlus 7 Pro camera, D_v is the distance between the virtual image and the camera lens, P_a is the area of a single pixel on the OnePlus 7 Pro camera (in mm^2), and N is the number of pixels in the selected image-processing area. The overall magnifica-

tion (M_o) was used to compute the size of each pixel, enabling calculation of endothelial cell density.

$$M_o = M_s * \frac{f_c}{D_v} = 40 * \frac{4.755 \text{ mm}}{250 \text{ mm}}$$

$$\text{Area} = \frac{P_a * N}{M_o} = \frac{6.4 * 10^{-7} \text{ mm}^2 * N}{M_o}$$

$$\text{ECD (cells/mm}^2\text{)} = (\#\text{cells in image}) / \text{Area}$$

CV was computed by calculating the area of each cell and using the below equation, where μ represents the mean cell area (in pixels), T represents the total number of cells, and c_i represents the size of a specific cell (in pixels).

$$CV = \frac{1}{\mu} \sqrt{\frac{1}{T} \sum_{i=1}^T (c_i - \mu)^2}$$

Statistical Analysis

The data was analyzed using Python version 3.6 with packages scikit-learn and matplotlib. A paired Student's *t*-test and Bland-Altman analysis were conducted.¹¹ *P* values < 0.05 were considered statistically significant.

Additionally, linear regression was performed on the Bland-Altman plots to assess proportional bias. The independent variable was the mean measurement, and the dependent variable was the difference between the specular and smartphone measurements. The null hypothesis was defined as the coefficient for the mean measurement being zero, and a two-sided Wald Test was used to compute the *P* value.

Results

All 15 participants (30 eyes) in the study were healthy and did not have any known ocular diseases. The mean age of the participants was 29 ± 14 years, with a range from 19 to 72 years. The average number of cells analyzed by our smartphone algorithm was 185.56 ± 49.28 cells, and by the Tomy specular microscope was 239.86 ± 59.79 cells.

We compared the ECD, HEX, and CV computed by the Tomy specular microscope (-T) with those computed by the smartphone app (-S) by using paired two-sided *t*-testing. There was no significant difference in the mean ECD computed by the two devices. The mean ECD-T was 2799 ± 156 cells/mm², and the mean ECD-S was 2779 ± 166 cells/mm², with a mean difference of 20 cells/mm² (*P* = 0.28). There was no significant difference in the mean HEX computed by the two devices. The mean HEX-T was $52 \pm 6\%$, and the mean HEX-S was $53 \pm 6\%$, with a mean difference of 1% (*P* = 0.50). There was a significant difference in the mean CV computed by the two devices. The mean CV-T was $34 \pm 3\%$ and the mean CV-S was $30 \pm 3\%$, with a mean difference of 3.8% (*P* < 0.01).

Bland-Altman plots are a widely used method to assess concordance between two instruments, and plots for ECD, HEX, and CV are provided in Figure 5. The plots show that 60% of our ECD-S measurements differed by fewer than 100 cells/mm² from the ECD-T. Similarly, 73% of HEX measurements had a smaller than 5% difference, and 96% of HEX measurements differed by less than 10%. Lastly, 70% of CV measurements had a smaller than 5% difference, and 97% of CV measurements differed by less than 10%. These data confirm that there is high concordance between ECD, HEX, and CV values as computed by the Tomy and our smartphone-based approach.

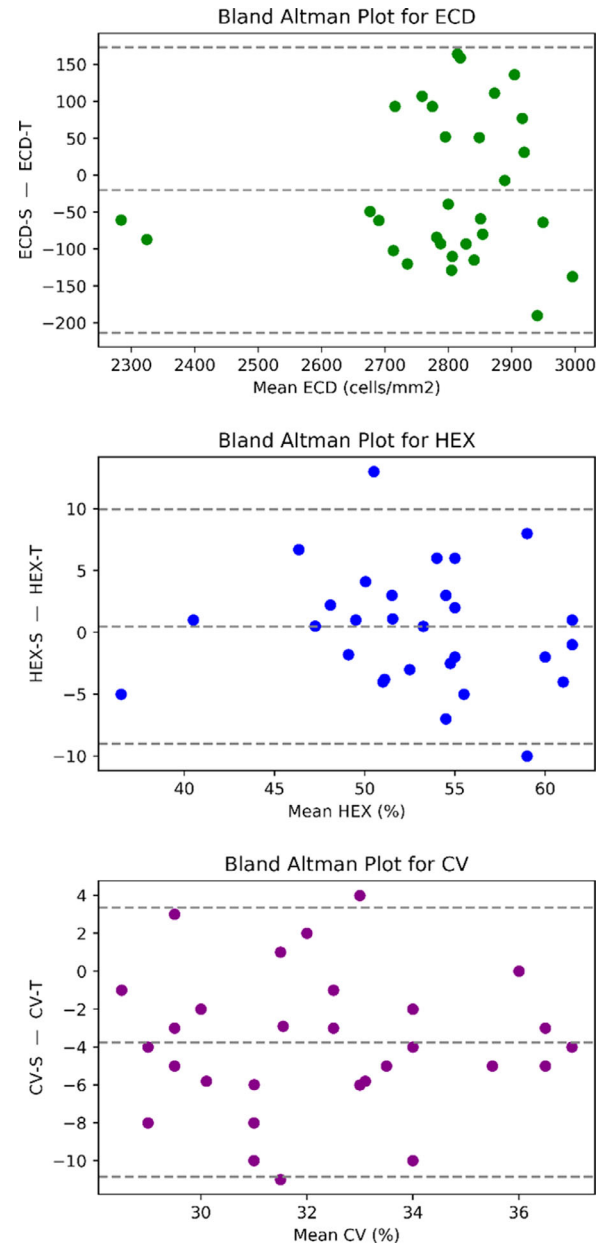


Figure 5. Bland-Altman analysis comparing results from smartphone-based imaging and Tomy specular microscope. The x-axis is the difference between the two measurements and the y-axis is the mean of the two measurements. The upper and lower dotted lines represent the 95% confidence interval. (A) Comparison of smartphone-computed endothelial cell density (ECD-S) and Tomy-computed endothelial cell density (ECD-T). (B) Comparison of smartphone-computed percentage of hexagonal cells (HEX-S) and Tomy-computed percentage of hexagonal cells (HEX-T). (C) Comparison of smartphone-computed cell variation (CV-S) and Tomy-computed cell variation (CV-T).

Linear regression was performed on the Bland-Altman plots to assess proportional bias. No proportional bias for ECD, HEX, and CV (*P* values 0.58, 0.65, and 0.90, respectively) was found, indicating

that the magnitude of the measurement is not correlated with the bias between the instruments.

Discussion

Our study demonstrates that smartphone-based imaging and analysis of the CE generates results comparable to those of traditional specular microscopy methods, providing a novel and low-cost tool for assessing CE function.

The mean ECD-T, HEX-T, and CV-T are very similar to those from previous studies, which also imaged healthy subjects using the Tomey EM-4000 specular microscope.^{12,13} We found no significant difference between the ECD and HEX values computed by our smartphone-based algorithm and those provided by the Tomey specular microscope. Our Bland-Altman regression analysis demonstrated no proportional bias for all three measurements. We did find a statistically significant difference in the CV computed by the smartphone-based method and the Tomey specular microscope. However, previous studies have compared non-contact specular microscopes and have shown that there are statistically significant differences between device measurements of ECD, HEX, and CV.^{14,15}

Specifically, Gasser et al. compared the performance of the Topcon SP3000P and Konan Noncon Robo SP800 by imaging 34 healthy eyes and found that there was a statistically significant difference between the device measurements of ECD and CV. Similarly, Karaca et al. imaged 50 healthy eyes to compare the Nidek CEM-530 and Konan CellCheckXL and also found a statistically significant difference between device measurements of ECD and CV. Thus, the concordance we achieved between our smartphone-based method and the Tomey instrument is comparable to the concordance between clinically approved specular microscopes.

Previous studies have described smartphone-based endothelial imaging but did not pursue the use of an automated analysis pipeline. Our image acquisition protocol is optimized for the use of image processing algorithms by standardizing camera settings, such as ISO and shutter speed. By keeping these factors the same between all patients, we were able to reliably and reproducibly image the endothelium of both eyes. The only factor that had to be adjusted in each session was the smartphone's manual focus in order to compensate for the patient's head movement. Furthermore, it took 2 to 4 minutes to image and analyze both eyes on the

smartphone device, which was similar to the speed of specular microscopy.

Additionally, all image analysis was performed in under 5 seconds on a mid-range Android smartphone, without the need for an internet connection or cloud computing services. Our image processing pipeline had robust performance across all images analyzed and was able to automatically compute clinically relevant parameters (ECD, HEX, and CV) commonly used for monitoring endothelial health. To our knowledge, our work is the first to demonstrate that fully automated analysis of smartphone-acquired corneal endothelium images is possible and generates results concordant with the analysis done by specular microscopes.

Our study illustrates the feasibility and accessibility of automated smartphone-based imaging and analysis of the CE. We leveraged a \$500 smartphone and a \$10 plastic attachment to image the CE at subcellular resolution. Commercial specular microscopes cost between \$25,000 and \$30,000 and are typically only available in tertiary-care facilities.¹⁶ Meanwhile, the slit-lamp is nearly ubiquitous in all ophthalmological clinics around the world, and over 90% of healthcare workers in many countries own smartphones.¹⁷ Moreover, many hospitals in developing countries conduct outreach eye-camps, where slit-lamps are brought into a rural field setting to assess patients.¹⁸ This technology would enable mobile, field-screening of endothelial health in the absence of traditional specular microscopes. This smartphone-based approach also has utility in pre-operative screening prior to intraocular surgery, where measurement of ECD provides an important risk assessment for surgical planning. Loss of corneal endothelial cells during intraocular surgery, most commonly cataract surgery, leads to pseudophakic bullous keratopathy, which is currently the leading indication for corneal transplantation.¹⁹ Furthermore, the inexpensive nature of this technique enables regular monitoring of ECD post-keratoplasty (PKP, DMEK, and DSAEK) in resource-limited settings.

The current limitations of this method include the requirement of a slit lamp with adequate magnification (32× or 40×) and the technical skill needed to obtain images. In the future, an auto-focus algorithm could be implemented to improve the ease-of-use of this technology. Furthermore, whereas we demonstrated high performance by using an image-processing pipeline with the KH algorithm to segment the smartphone images, additional image-processing methods could be explored and evaluated.

Although our study demonstrates the promise of this method, it has a relatively small sample size of 30 eyes, which may limit the generalizability and

statistical significance of the results. Future studies with a larger patient sample size, including patients with ocular diseases, such as FECD, are required to further validate this technology. Preliminary data indicate that this technique can be used to image the CE in patients with FECD, yielding results comparable to those obtained from specular microscopy (Supplementary Fig. S1). In addition, because the slit-lamp can be manually steered, our method could enable imaging of any central or peripheral region of the CE, rather than solely the 4 to 6 discrete regions imaged by commercial specular microscopes.

Overall, smartphone-based imaging is a promising low-cost technique that can assess the corneal endothelial status of healthy patients, with the potential to screen for endothelial disorders and identify patients at risk for complications before and after intraocular surgery. Our study demonstrates that this method produces results concordant with those of a modern specular microscope, validating the performance of our novel image processing pipeline. The platform we developed is a fraction of the cost of current specular microscopes, is portable, and does not require an internet connection. This technology could enable regular endothelial screening in under-resourced communities, mitigating health disparities in eye care.

Acknowledgments

The authors thank the participants of this study for their time. The authors thank Gumv Prasad and Venkatesh Lakkireddy from the Sri Kiran Institute of Ophthalmology for their assistance in imaging patients and thank the advisory board of the Global Alliance for Medical Innovation (GAMI) for their thoughtful feedback.

Disclosure: **S. Mantena**, None; **J. Chandra**, None; **E. Pecyna**, None; **A. Zhang**, None; **D. Garrity**, None; **S. Ong Tone**, None; **S. Sastry**, None; **M. Uddaraju**, None; **U.V. Jurkunas**, None

* SM and JC contributed equally to this paper.

References

1. Bourne WM. Biology of the corneal endothelium in health and disease. *Eye (Lond)*. 2003;17(8):912–918.
2. Musch DC, Niziol LM, Stein JD, Kamyar RM, Sugar A. Prevalence of corneal dystrophies in the United States: estimates from claims data. *Invest Ophthalmol Vis Sci*. 2011;52(9):6959–6963.
3. Edelstein SL, DeMatteo J, Stoeger CG, MacSai MS, Wang CH. Report of the Eye Bank Association of America Medical Review Subcommittee on Adverse Reactions Reported from 2007 to 2014. *Cornea*. 2016;35(7):917–926.
4. Ong Tone S, Jurkunas U. Imaging the corneal endothelium in Fuchs corneal endothelial dystrophy. *Semin Ophthalmol*. 2019;34(4):340–346.
5. National Coverage Determination (NCD) for Endothelial Cell Photography (80.8). Available at: <https://www.cms.gov/medicare-coverage-database/details/ncd-details.aspx?NCDId=213&ncdver=1&bc=AAAQAAAAAA&>. Accessed November 25, 2020.
6. Toslak D, Thapa D, Erol MK, Chen Y, Yao X. Smartphone-based imaging of the corneal endothelium at sub-cellular resolution. *J Mod Opt*. 2017;64(12):1229–1232.
7. Fliotsos MJ, Deljookorani S, Dzhaber D, Chandan S, Ighani M, Eghrari AO. Qualitative and quantitative analysis of the corneal endothelium with smartphone specular microscopy. *Cornea*. 2020;39(7):924–929.
8. Piorkowski A, Nurzynska K, Gronkowska-Serafin J, Selig B, Boldak C, Reska D. Influence of applied corneal endothelium image segmentation techniques on the clinical parameters. *Comput Med Imaging Graphics*. 2017;55:13–27.
9. Daniel MC, Atzrodt L, Bucher F, et al. Automated segmentation of the corneal endothelium in a large set of ‘real-world’ specular microscopy images using the U-Net architecture. *Sci Rep*. 2019;9(1):4752.
10. Fabijańska A. Segmentation of corneal endothelium images using a U-Net-based convolutional neural network. *Artif Intell Med*. 2018;88:1–13.
11. Martin Bland J, Altman DG. Statistical methods for assessing agreement between two methods of clinical measurement. *Lancet*. 1986;1(8476):307–310.
12. Kosekahya P, Ucgul Atilgan C, Atilgan KG, et al. Corneal endothelial morphology and thickness changes in patients with gout. *Turk J Ophthalmol*. 2019;49(4):178–182.
13. Szalai E, Nemeth G, Berta A, Modis LJ. Evaluation of the corneal endothelium using non-contact and contact specular microscopy. *Cornea*. 2011;30(5):567–570.
14. Gasser L, Reinhard T, Böhringer D. Comparison of corneal endothelial cell measurements by two non-contact specular microscopes. *BMC Ophthalmol*. 2015;15:87.

15. Karaca I, Yilmaz SG, Palamar M, Ates H. Comparison of central corneal thickness and endothelial cell measurements by Scheimpflug camera system and two noncontact specular microscopes. *Int Ophthalmol*. 2018;38(4):1601–1609.
16. Bonnell AJ, Cymbor M. Under the specular microscope. *Review of Optometry*. 2012;149(8):58–65.
17. Mobasher MH, King D, Johnston M, Gautama S, Purkayastha S, Darzi A. The ownership and clinical use of smartphones by doctors and nurses in the UK: a multicentre survey study. *BMJ Innov*. 2015;1(4):174–181.
18. Farooqui JH, Jorgenson R, Gomaa A. Mobilizing slit lamp to the field: a new affordable solution. *Indian J Ophthalmol*. 2015;63(11):864–867.
19. Eye Bank Association of America Statistical Report 2019. Eye Bank Association of America. Published 2019, <https://restoresight.org/what-we-do/publications/statistical-report>. Accessed February 2, 2021.